A Structural and Vibrational Study of Uranium(III) Molecules by Density Functional Methods

Laurent Joubert and Pascale Maldivi*

Laboratoire de Reconnaissance Ionique, Service de Chimie Inorganique et Biologique (UMR 5046 CEA-CNRS-UJF), Département de Recherche Fondamentale sur la Matière Condensée, CEA-Grenoble, 17 rue des Martyrs, 38054 Grenoble Cedex 9, France

Received: June 18, 2001; In Final Form: July 14, 2001

In this paper, we present a theoretical investigation of structural and vibrational properties of selected gas-phase UX_3 (X = F, Cl, Br, and I) and $U(CH_3)_3$ molecules by density functional methodologies or with a post Hartree−Fock MP2 perturbative approach. Relativistic scalar corrections have been explicitly included either by a frozen core approximation with a quasi-relativistic treatment (QR) of the valence electron shells or by energy-adjusted large core quasi-relativistic effective core potential (QRECP) scheme. The influence of the size of the core (large core, LC, or small core, SC) as well as of the addition of polarization functions has also been examined on one derivative, i.e., UCl_3. MP2/LC-QRECP optimized geometries and vibrational frequencies are found in good agreement with the available estimated or experimental data. Among the different DFT approaches, the best agreement is obtained for DFT/QR computations which reproduce the experimental (or estimated) C_{3v} molecular structures of all the selected species. In contrast, the DFT/LC-QRECP approaches provide irregular results, strongly dependent on the choice of the functional. Nevertheless, the use of a small core pseudopotential greatly reduces the margin between MP2 and DFT/QRECP calculations. At this level, both "classical" nonlocal gradient corrected and hybrid density functionals provide reasonable results. The only exception concerns the B3LYP functional that is clearly inadequate for an effective treatment of electron correlation in open-shell molecular systems.

1. Introduction

In the past decades, the chemistry of very heavy metals has been the subject of various and numerous experimental and theoretical investigations.[1−3] An important and particular aspect of this topic concerns the study of lanthanide− or actinide− ligand interactions for molecules involved in the nuclear waste disposal. In this context, there is a need for theoretical modeling and recently, various molecular dynamics,[4−6] ab initio,[6−16] and density functional theory (DFT) studies[16−27] have focused on the structural studies of large or small model molecular systems involved in extraction processes relevant to the nuclear industry. But a theoretical treatment of such species still represents a challenging task for modern quantum mechanics methods. Besides the well-known intrinsic difficulty of open-shell system calculations, an efficient treatment of relativistic and correlation effects has to be chosen.

Since the development of accurate density functionals including gradient corrections and more recently a part of exact exchange, the DFT approach has proven to be a powerful alternative to the classic Hartree−Fock (HF) or post-HF methods for transition metal studies, in addition to a lesser computational effort.[28] Moreover, different approximations allow to take into account the main relativistic effects (mass−velocity and Darwin terms) within a DFT formalism, such as the use of relativistic effective core potentials[8] (RECP) or by a fully relativistic frozen core description combined with a perturbational scalar quasi-relativistic (QR) treatment of valence shells.[29−31] In particular, these methodologies have recently been successfully applied to the study of lanthanide trihalide systems for which experimental data are available.[17−19,23] The reproduction of experimental data was shown to be at least of the same quality or better, than post-HF/RECP methodologies.

Our purpose is to investigate the reliability and the accuracy of these methodologies for 5f elements. More precisely, we will focus on the structural and vibrational properties of small reference uranium(III) complexes, i.e., UX_3 (X = F, Cl, Br, I) and $U(CH_3)_3$ molecules. Moreover, post-HF calculations can be also reasonably considered for these small molecular systems. Thus we decided to perform also MP2 calculations, to compare with the DFT computations, as DFT/post-HF comparisons had already been made for LnX_3 species.[17,18] More accurate post-HF methods (MP4 and CCSD) have been attempted but they appeared to be too demanding in computer resources to be applied to such high spin unrestricted species (see below).

The various quasi-relativistic/DFT methodologies that are described here involve:

- gradient corrected (GGA) exchange and correlation functionals in combination with a frozen core and a Pauli or ZORA treatment (see details in the computational section);

- a GGA exchange and correlation functional or self-consistent hybrid (SCH) functionals, including some exact exchange, combined with a large core (LC) RECP for the treatment of relativistic effects.

More accurate calculations have also been carried out on UCl_3 to assess both the quality of the LC approximation (comparison with small core RECP calculations) and the influence of extended polarization functions on halogen atoms.

2. Computational Details

Two different implementations of the Kohn−Sham (KS) methodology have been used to take into account the relativistic

* Corresponding author. E-mail: Pmaldivi@cea.fr.

10.1021/jp012301g CCC: $20.00
Published on Web 09/07/2001

effects. In the first one, a scalar quasi-relativistic (QR) approach has been chosen,[29−31] as developed in the Amsterdam Density Functional[32−35] (ADF1999.02) package, where the atomic core electronic density is obtained via a fully relativistic Dirac Slater (DS) calculation. The valence wave function is derived from a quasi first-order perturbative treatment of the mass−velocity and Darwin main relativistic terms, constituting the so-called Pauli approximation. To check the adequacy of the core-valence separation model, the zeroth-order regular approximation (ZORA) Hamiltonian was also employed,[31] ensuring the variational stability of the wave function in the core region where the expansions that lead to the Pauli Hamiltonian are no longer valid. The valence space includes the $6s^2 6p^6 5f^5 6d^1 7s^2$, $2s^2 2p^2$ and $ns^2 np^5$ electrons for uranium, carbon, and halogens, respectively. It was described by nonrelativistic triple-ζ Slater Type Orbitals (STO) basis sets. One single d polarization function was added for carbon and halogens.[36] Auxiliary sets of STO functions were used for all the atoms to fit the molecular density and to generate the Coulomb and exchange potentials.[37]

The second relativistic approach, as developed in the Gaussian 98[38] package, is based on the use of energy-consistent quasi-relativistic effective core potentials (QRECP) developed by the Stuttgart−Dresden−Bonn group.[8,39−40] This approach consists of replacing the inner core shell electrons of heavy atoms by a pseudopotential adjusted to reproduce valence energies computed by all-electron quasi-relativistic Wood-Boring computations.[41] The corresponding valence space of the uranium atom treats explicitly the outer core and valence shells (6s, 6p, 5f, 6d, and 7s electrons), referring as a large core (LC) QRECP.[39] This pseudopotential has been chosen to allow systematic comparisons with the scalar quasi-relativistic approach of ADF, replacing 78 core electrons. This corresponds to a contracted Gaussian Type Orbital (GTO) basis set with a (8s8p6d5f2g)/[5s5p4d3f2g] contraction scheme. The $ns^2 np^5$ valence shell of the halogens has been taken into account, described by a contracted (4s5p1d)/[2s3p1d] GTO polarized basis set.[40] This QRECP scheme has been also employed to perform the MP2[42] calculations. A complementary study has been carried out on UCl_3, employing a small core (SC) pseudopotential on uranium (60 electrons) with a (12s11p10d8f)/[8s7p6d4f] contraction scheme for the nonrelativistic treatment of the outer core and valence shells.[39] Furthermore, the influence of additional polarization functions (3df) on chlorine atoms has been explored.[43] Finally, light atoms, i.e., carbon and hydrogen elements, were described by all electron 6-31G(d,p) GTO basis sets.[44]

Two different schemes were employed to describe the exchange and correlation potentials in DFT calculations. In the first approach, based on the generalized gradient approximation (GGA), we have considered the exchange and correlation functionals of Becke 88[45] (B) and Perdew 86[46] (P), respectively. The choice of this exchange−correlation functional (BP) is based on a previous theoretical work which clearly emphasized the adequacy of this functional in reproducing experimental results for similar 4f metal compounds.[18] The second approach is based on the so-called self-consistent hybrid (SCH) methodology,[47,48] introducing an "a priori" fixed Hartree−Fock exchange ratio within the exchange potential. We used the three-parameter hybrid functional of Becke[47] (B3), combined with either the Perdew (P) or the Lee−Yang−Parr (LYP)[49] functional and the "parameter free" hybrid model[48] issuing from the Perdew−Burke−Ernzerhof (PBE) exchange−correlation functional[50,51] (hereafter PBE0). It is important to note that the LYP correlation functional, long-considered as a reference for DFT calculations on organic systems, may be inadequate for heavier atomic or molecular systems, especially open-shell metal complexes, as evidenced by recent theoretical studies on both third-row non transition elements[52] and different metal complexes,[18,23,53,54] whereas it is able to give reliable results for closed-shell heavy metals such as in uranyl derivatives.[15,16] This may be due to the fact that the LYP functional does not distinguish the correlation between electrons of parallel spins and the correlation between electrons of antiparallel spins. To check this point for our present heavy molecular systems, we decided to include this functional in our calculations.

One important point concerns the open-shell nature of these species. The ground electron configuration of U(III) is $5f^5$ which by application of Hund's rule, would lead to a ground quartet state. In molecular species such as the trihalides, the interaction is expected to be mainly electrostatic and the 5f orbitals are not strongly involved in the bonding (see the results below which support this assumption). Crystal field splitting effects are supposed to be weak: to give an order of magnitude, the crystal field splitting of U^{3+} diluted in $LaCl_3$ is 451 cm^{-1}.[55] Moreover, magnetic susceptibility measurements performed on trivalent uranium halides have shown an effective magnetic moment of ca. 3.6−3.7 μ_B at room temperature,[56] thus close to the spin-only value of a $S = 3/2$ spin (3.87 μ_B). Complete active space (CAS-SCF) calculations[57] performed on $U(CH_3)_3$ have also shown the existence of a manifold of low-lying excited states arising from all possible excitations of the three high spin electrons among the 5f-type orbitals. From these considerations, we have performed our calculations with the maximum spin polarization (number of spin α electrons minus number of spin β electrons) corresponding to a quartet state, i.e., 3, in the unrestricted KS formalism. Moreover, the spin−orbit coupling has not been explicitely included in the present study, because it should merely mix together the states in the manifold issued from the $5f^5$ configurations. The molecular properties should therefore not be affected and this assumption was also verified by Ortiz and co-workers,[57] pointing out small spin−orbit coupling effects for $An(CH_3)_3$ species (An = U, Np, and Pu). In fact, our computations performed in C_{3v} symmetry group lead to a $^4A_1$ ground state.

Finally, all the geometries have been fully optimized starting from both pyramidal (C_{3v}) and planar (D_{3h}) conformations, using either an analytical gradient driven procedure with an "ultrafine" grid for numerical integration (Gaussian 98) or with a high numerical integration parameter (i.e., 7.0) for ADF 99. The nature of the optimized structures have been checked by evaluation of the harmonic frequencies.

3. Results and Discussion

Uranium Trihalide Molecules. From an experimental point of view, the amount of structural and spectroscopic data on gaseous actinide(III) trihalide species is very limited in the literature.[58−63] High-temperature electron diffraction (ED) studies have been reported by Bazhanov and co-workers,[58−60] allowing to derive thermal-averaged molecular structures for UCl_3 and UI_3 species. From the vibration amplitudes thus obtained, they calculated the wavenumbers of the vibrational spectra of the UCl_3 and UI_3 molecules. More recently, Kovács et al. measured the first high-temperature infrared (IR) spectrum of the gas phase above a solid sample of UCl_3, assigning the different bands to both UCl_3 and UCl_4 species.[62] Some estimates of molecular properties (primarily spectroscopic and molecular constants) have also been proposed for uranium trihalide molecules, tabulated by analogy with those of other heavy metal trihalide molecules.[62,63]

TABLE 1: Calculated and Experimental Bond Lengths (r in Å) and Bond Angles (θ in degrees) of UX_3 Molecules (QRECP results include only LC computations)

	UF_3		UCl_3		UBr_3		UI_3	
	r	θ	r	θ	r	θ	r	θ
BP/QR/Pauli	2.051	108.8	2.508	108.9	2.667	110.3	2.926	111.4
BP/QR/ZORA	2.063	107.4	2.524	109.6	2.686	109.8	2.912	111.0
BP/QRECP	2.121	113.0	2.592	115.7	2.753	118.7	2.981	120.0
B3P/QRECP	2.106	111.8	2.575	114.6	2.734	118.0	2.958	120.0
B3LYP/QRECP	2.122	118.4	2.592	114.5	2.760	118.2	2.986	120.0
PBE0/QRECP	2.096	115.3	2.565	109.5	2.730	117.5	2.954	119.2
MP2/QRECP	2.083	104.7	2.521	106.9	2.661	107.2	2.881	108.6
exptl[a]			2.549 ± 0.008	95 ± 3			2.88 ± 0.01	89 ± 3

[a] Refs 58 and 60.

In a first step, we decided to calculate optimized molecular parameters for the whole series of UX_3 complexes (X = F, Cl, Br, and I) and we compared our computed structural results with all the available data, either experimentally measured[58−60] or estimated.[62,63] It is of prime importance to note that the comparisons between experimental and computed geometrical parameters must be made with caution. As it has been emphasized in a recent review focused on the molecular structures of metal halides,[64] several problems arise from ED studies. For example, the high temperature conditions and the anharmonicity of the vibrations lead to thermal-averaged structures, which may be quite different from the calculated equilibrium geometries of a motionless molecule, a problem which is certainly emphasized by the "floppy" character of these complexes. Moreover, in the case of estimated geometrical parameters, the attempted analogy with other heavy metal halides (mainly lead and bismuth halides) also leads to hazardous comparisons. Nevertheless, in the absence of experimental equilibrium structures, we chose to compare our results to the existing tabulated values.

In Table 1, are listed the optimized geometrical features of these molecules, i.e., the U−X bond lengths and the X−U−X bond angles (θ), calculated by DFT and MP2 methods, at the LC level for QRECP computations, together with the available ED measurements. Although a quantitative comparison between experimental and theoretical bond angles could be hazardous, qualitative trends can be examined. In particular, both experimental and theoretical bond angles indicate that the UX_3 molecules prefer a pyramidal C_{3v} arrangement.

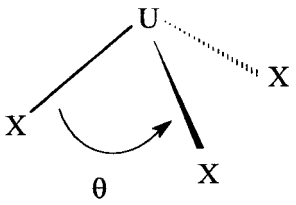

In going from the fluoride to the iodide complex, we can expect, merely by steric considerations, an increase in the bond angle θ tending toward a planar geometry. Such a trend is observed at the BP/QR and by most of QRECP levels, except for the B3LYP and PBE0 functionals, but is not confirmed by the experimental bond angles. On the contrary, the ED angles show a strong pyramidalization, with a slightly decrease of θ (i.e. −6°) from Cl to I. This pyramidalization is well reproduced, but to a lesser extent, by BP/QR or MP2/QRECP calculations which indicate a C_{3v} structure for both complexes. Anyway, as stated before, angular data must not be considered as significant parameters to compare computational methods.

To estimate the floppy character of these molecules, we have computed the energy cost between C_{3v} and D_{3h} conformations. Geometry optimizations in the planar geometry were carried out at the MP2/LC-QRECP level, and the energy difference (ΔE) with C_{3v} optimized structures was calculated including the zero-point energy correction (ZPE). The highest ΔE value, ∼19 kJ/mol is obtained for UF_3, whereas other values range from 5 kJ/mol (UCl_3) to 11 kJ/mol (UI_3) and to 13 kJ/mol (UBr_3). Such low values clearly show the flexibility of these molecules, although less pronounced than in the lanthanide homologues LnX_3, where ΔE values were close or less than 5 kJ/mol.[18]

The analysis of the experimental and theoretical metal−ligand bond lengths is thus more significant to compare the performance of the various computations. The first trend concerns the substantial increase in going from fluoride to iodide complexes. Only very small deviations are observed between the different levels of theory. Moreover, if we consider as a reference the experimental lengthening from U−Cl to U−I bond (+0.33 Å), the calculated mean deviation equals to 0.06 Å. Therefore, we can estimate a mean lengthening, which equals +0.46 Å from F to Cl, +0.16 Å from Cl to Br, and +0.23 Å from Br to I. These results are very close to the bond lengthening observed for lanthanide trihalide molecules, i.e., +0.46 Å from F to Cl, +0.15 Å from Cl to Br, and +0.21 Å from Br to I. These variations do not depend on the nature of the metal atom and, moreover, they are very similar to the changes of the ionic radius for the halides,[65] i.e. +0.48 Å from F^- to Cl^-, +0.15 Å from Cl^- to Br^-, and +0.24 Å from Br^- to I^-, suggesting that the bonding either in Ln(III) trihalides or in U(III) trihalides is mainly ionic.

Let us now take a closer look at the differences between experimental and theoretical values for the chloride and iodide species. We first note a very good agreement, the best of all our computations, between experimental and MP2 calculated bond lengths, characterized by a mean deviation below 0.02 Å. Among the various DFT approaches, the Pauli and ZORA quasi-relativistic calculations provide the best agreement with the available ED bond lengths, the corresponding mean deviations being 0.04 and 0.03 Å, respectively. If we then adopt a QRECP scheme, similar agreements are obtained with the PBE0 and B3P density functionals, with 0.04 and 0.05 Å mean deviations, respectively. Other exchange−correlation functionals, i.e., BP and B3LYP functionals, indicate reasonable but less accurate bond length estimations corresponding to higher mean deviations, i.e., ∼0.07 Å.

Further comparisons can be made from estimated molecular structures based on the corresponding products of molecular inertia moments, which have been reported by several authors.[62,63] Table 2 presents a series of estimated and MP2 or DFT calculated values. It is worth noting that the masses of the ligands as well as the overall molecular structure strongly influence the inertia moments values (see Figure 1). On one

TABLE 2: Calculated and Estimated Products of Molecular Inertia Moments (in g^3 cm^6) of UX_3 Molecules

	UF_3 $I_AI_BI_C*10^{113}$	UCl_3 $I_AI_BI_C*10^{113}$	UBr_3 $I_AI_BI_C*10^{113}$	UI_3 $I_AI_BI_C*10^{113}$
BP/QR (Pauli)	2	32	493	3466
BP/QR (ZORA)	2	33	511	3345
BP/QRECP	2	40	660	4443
B3P/QRECP	2	38	624	4241
B3LYP/QRECP	2	40	661	4488
PBE0/QRECP	2	37	615	4157
MP2/QRECP	2	33	468	3008
estimated[a]	1	37	488	2880

[a] Refs 62 and 63.

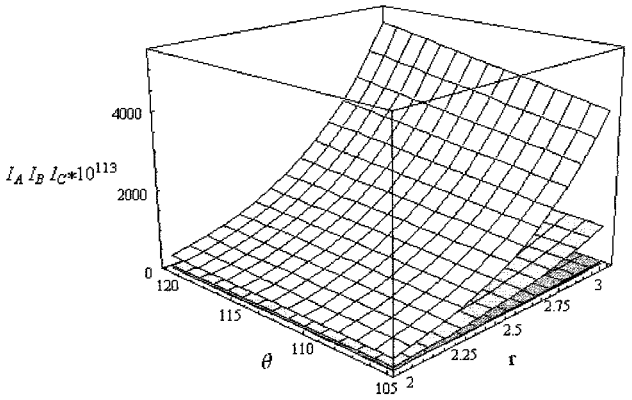

Figure 1. Evolution of the product of the molecular inertia moments (in g^3 cm^6) of UX_3 molecules versus bond length (r in Å) and bond angle (θ in degrees). From dark gray to light gray: UF_3, UCl_3, UBr_3, and UI_3.

hand, the estimated and calculated inertia moment products of the uranium trifluoride and trichloride molecules are almost constant. On the other hand, small structural differences between the estimated and calculated geometries of the tribromide or triiodide complexes lead to substantial and irregular deviations between the corresponding inertia moment products. For example, a 0.1 Å bond length deviation with a fixed 110° bond angle corresponds to a 7.0×10^{-111} g^3 cm^6 deviation (24%) of the inertia moment product of UI_3. For the same molecule, a 10° bond angle deviation with a 2.88 Å fixed bond length corresponds to a 5.4×10^{-111} g^3 cm^6 deviation (19%) of this product. A systematic comparison between the different levels of theory is therefore difficult. Nevertheless, we can compare, for each theoretical approach, a total deviation of the calculated values from the estimated data, summed over the four selected species. A minimal total deviation of 1.5×10^{-111} g^3 cm^6 is obtained for MP2 results. This relatively small total deviation indicates a strong analogy between the MP2 calculated and the estimated equilibrium structures. For DFT/QR calculated structures, the resulting total deviation is still satisfactory, being equal to 6.0×10^{-111} and 5.0×10^{-111} g^3 cm^6 for Pauli and ZORA calculations, respectively. The other values (QRECP calculations) are all beyond 1.0×10^{-110} g^3 cm^6: i.e., 1.4×10^{-110} (PBE0), 1.5×10^{-110} (B3P), 1.7×10^{-110} (BP), and 1.8×10^{-110} g^3 cm^6 (B3LYP).

From all these observations, we decided to choose the MP2 calculated geometries as the reference optimized structures. Therefore, the bond length absolute mean deviations between DFT and MP2 results have been calculated (see Figure 2). The best results have been obtained for DFT/QR calculations, with a mean deviation varying between 0.02 (ZORA) and 0.03 Å (Pauli). The other results confirm the tendency previously obtained. For all DFT/QRECP calculations, the mean deviation

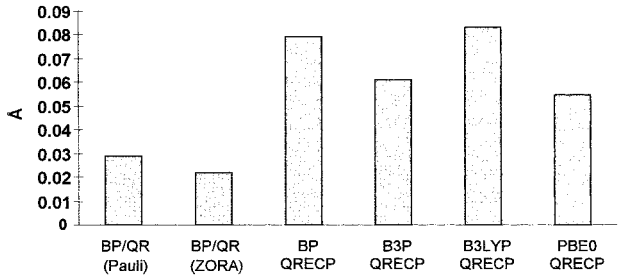

Figure 2. Absolute mean deviations (in Å) between DFT and MP2 bond lengths of UX_3 molecules.

is higher than 0.05 Å, the best agreement being obtained for the PBE0/QRECP approach.

In Table 3 are collected the calculated harmonic wavenumbers together with experimental[58−61] or estimated[62,63] ones. The four normal modes correspond to the symmetric stretching (ν_1), out-of-plane bending (ν_2), antisymmetric stretching (ν_3), and in-plane bending modes (ν_4). It is important to remember that the estimated values are extrapolated from spectroscopic data of other heavy metal trihalide molecules. Let us focus on these estimated spectroscopic data, which are available for all the selected molecular species. Figure 3 represents the mean deviations observed between each of the calculated and estimated wavenumbers. The lowest deviations correspond to the symmetric stretching mode, within a range of 9−31 cm^{-1}. These small deviations are directly related to the general good agreement observed between calculated and experimental (or estimated) bond lengths. On the opposite side, the highest deviations (27−54 cm^{-1}) correspond to the out-of-plane bending mode, especially for molecules containing heavy ligands, i.e., the bromide and iodide complexes. The strong anharmonicity of this mode and the difficulty to detect it from an experimental point of view could easily explain these discrepancies. However, we have to keep in mind that our comparison is based only on estimated data. We think therefore that the ν_2 wavenumber is certainly overestimated for UBr_3 and UI_3 molecules, indicating very fluxional and strongly pyramidalized complexes. As stated above, such a high pyramidalization is questionable, due to the strong steric repulsions between these bulky ligands.

From a more general point of view, we can estimate a mean deviation over all the wavenumbers. On one hand, the best agreements are obtained for DFT/QR and MP2/QRECP vibrational wavenumbers, with a mean deviation of 23 cm^{-1}(Pauli)/22 cm^{-1}(ZORA) and 26 cm^{-1}, respectively. On the other hand, highest deviations correspond to BP/QRECP and B3LYP/QRECP approaches, with a 37 cm^{-1} mean deviation for both of them. Among the experimentally measured values, it is worth noting that only the symmetric stretching band of gaseous UCl_3 was directly measured by Kovács and co-workers.[61] All other experimental data are derived from the ED measurements of Bazhanov et al.,[58,60] starting from the vibration amplitudes they obtained and assuming a simple force field for the selected species, i.e., the UCl_3 and UI_3 molecules. These ED derived frequencies are close to the estimated frequencies and can themselves be considered as "estimated" data. The experimentally measured stretching band of gas-phase UCl_3 is much more interesting. The high-temperature infrared spectrum of the vapor phase was measured above a solid UCl_3 sample. A band was therefore observed at 275 cm^{-1} and assigned to the stretching band of UCl_3. However, all the calculations indicate a ν_1 wavenumber higher than 300 cm^{-1}, in agreement with the estimated (325 cm^{-1}) or ED derived (300 cm^{-1}) values. The assignment of this band to UCl_3 is thus not so evident. Moreover,

TABLE 3: Calculated and Estimated or Experimental (ED or IR) Vibrational Wavenumbers (in cm^{-1}) of UX_3 Molecules

	UF_3				UCl_3				UBr_3				UI_3			
	ν_1	ν_2	ν_3	ν_4	ν_1	ν_2	ν_3	ν_4	ν_1	ν_2	ν_3	ν_4	ν_1	ν_2	ν_3	ν_4
BP/QR (Pauli)	577	86	559	104	321	59	322	69	202	40	220	43	141	29	164	31
BP/QR (ZORA)	559	90	546	106	318	56	320	65	202	31	204	53	147	30	171	31
BP/QRECP	536	73	500	107	305	30	300	55	183	14	208	35	128	11	164	20
B3P/QRECP	555	61	516	108	317	33	311	61	194	18	216	37	137	8	172	24
B3LYP/QRECP	534	41	504	104	308	30	304	59	189	18	210	38	133	12	167	26
PBE0/QRECP	550	59	520	112	324	48	312	72	195	20	217	37	138	11	172	26
MP2/QRECP	583	111	537	131	353	52	341	75	222	39	234	49	162	28	183	36
estimated[a]	600 ± 100	100 ± 50	550 ± 100	140 ± 50	325 ± 30	55 ± 10	315 ± 30	90 ± 10	200 ± 30	100 ± 10	170 ± 30	90 ± 10	150 ± 30	60 ± 10	140 ± 30	55 ± 10
exptl (ED)[b]					300 ± 30									50 ± 10		
exptl (IR)[c]					275.0 ± 0.5	90 ± 10	310 ± 30	90 ± 10					130 ± 15		155 ± 15	45 ± 10

[a] Refs 62 and 63. [b] Refs 58 and 60. [c] Ref 61.

Figure 3. Absolute mean deviations (in cm^{-1}) between calculated and estimated vibrational wavenumbers of UX_3 molecules.

another band at 338 cm^{-1} was assigned to the UCl_4 molecule. Due to the large width of this band, the two stretching bands of UCl_3, which are very close from this value and from each other, may well be masked. Finally, we have to notice that the two bending frequencies are too small to be detected by the spectrometer (75−375 cm^{-1} range). Matrix isolation measurements, which have been already successfully applied to the study of lanthanide trihalide molecules,[66,67] should be able to determine precisely the different vibration modes of this molecule.

The differences observed between DFT/QR and DFT/QRECP results led us to perform a complementary study to check both the quality of the LC approximation in our QRECP calculations and the influence of additional polarization functions on chlorine atoms. We focused on the case of the UCl_3 molecule for which both estimated and experimental data are available. A structural and vibrational analysis was therefore carried out. These results were then compared to the previously obtained data (see Table 1) and are summarized in Table 4. To make unambiguous statements about the relative performance of the various methods, we have chosen to compare them to the most accurate available method, i.e., MP2/QRECP-SC+3df(Cl). The histograms on Figure 4a and 4b give a graphical representation of such comparisons.

The size of the pseudopotential (SC or LC) has a strong influence on the DFT computed bond lengths. For example, a systematic comparison between LC-QRECP+3df(Cl) and SC-QRECP+3df(Cl) results points to substantial bond shortenings, varying from 0.032 Å (PBE0) to 0.068 Å (BP). This effect is much more pronounced for the GGA functional BP, than for the hybrid functionals. In turn, it is clear also that the core size has more influence on DFT results than on MP2 results. Finally, we observe that the use of a SC improves the performance of B3LYP, but the predicted distances are still farther from experimental ones than with other DFT computations, for a given basis set. Irregular bond angle decreases are observed, i.e., less than 1° for hybrid functionals and more than 8° for the GGA functional BP. These bond length and bond angle variations are corroborated by the vibrational analysis that exhibits small wavenumber absolute mean deviations, except for BP (17 cm^{-1}). More generally, the performance for the computation of harmonic wavenumbers among the various methodologies, when using a SC instead of a LC, follow the same trends as for bond lengths. Clearly, we can notice a general better agreement between post Hartree−Fock and DFT results for both hybrid and GGA functionals. The only exception concerns the B3LYP functional, thus confirming the trends observed with a LC approximation.

The whole results are in excellent agreement with the estimated wavenumbers, except for the in-plane bending mode (ν_4) which was certainly overestimated by Hildenbrand and coworkers.[63] The reproduction of the structural data is less clear,

TABLE 4: Calculated Structural Parameters (bond lengths r in Å and bond angles θ in degrees) and Vibrational Wavenumbers (ν_1, ν_2, ν_3 and ν_4 in cm^{-1}) of UCl_3: Influence of the Size of the Uranium Pseudopotential (large or small core) and Additional Polarization Functions (3df) on Chlorine Atoms

	r	θ	ν_1	ν_2	ν_3	ν_4
BP/QR/Pauli	2.508	108.9	321	59	322	69
BP/QR/ZORA	2.524	109.6	318	56	320	65
BP/QRECP-LC	2.592	115.7	305	30	300	55
BP/QRECP-LC+3df(Cl)	2.591	116.5	305	29	302	56
BP/QRECP-SC	2.531	108.3	319	52	320	70
BP/QRECP-SC+3df(Cl).	2.523	108.3	319	52	320	70
B3P/QRECP-LC	2.575	114.6	317	33	311	61
B3P/QRECP-LC+3df(Cl)	2.567	110.0	323	48	314	80
B3P/QRECP-SC	2.537	109.9	328	47	326	68
B3P/QRECP-SC+3df(Cl)	2.525	109.2	325	50	325	71
B3LYP/QRECP-LC	2.592	114.5	308	30	304	59
B3LYP/QRECP-LC+3df(Cl)	2.594	111.1	313	47	301	64
B3LYP/QRECP-SC	2.564	111.0	316	45	315	67
B3LYP/QRECP-SC+3df(Cl)	2.553	110.5	316	48	315	70
PBE0/QRECP-LC	2.565	109.5	324	48	312	72
PBE0/QRECP-LC+3df(Cl)	2.561	109.8	323	48	314	71
PBE0/QRECP-SC	2.539	110.2	326	47	325	67
PBE0/QRECP-SC+3df(Cl)	2.529	109.8	324	48	324	70
MP2/QRECP-LC	2.521	106.9	353	52	341	75
MP2/QRECP-LC+3df(Cl)	2.510	107.1	338	52	339	70
MP2/QRECP-SC	2.513	106.3	335	62	338	81
MP2/QRECP-SC+3df(Cl)	2.508	105.8	333	58	334	68
estimated[a]			325 ± 30	55 ± 10	315 ± 30	90 ± 10
exptl (ED)[b]	2.549 ± 0.008	95 ± 3	300 ± 30	90 ± 10	310 ± 30	90 ± 10
exptl (IR)[c]			275.0 ± 0.5			

[a] Refs 62 and 63. [b] Refs 58 and 60. [c] Ref 61.

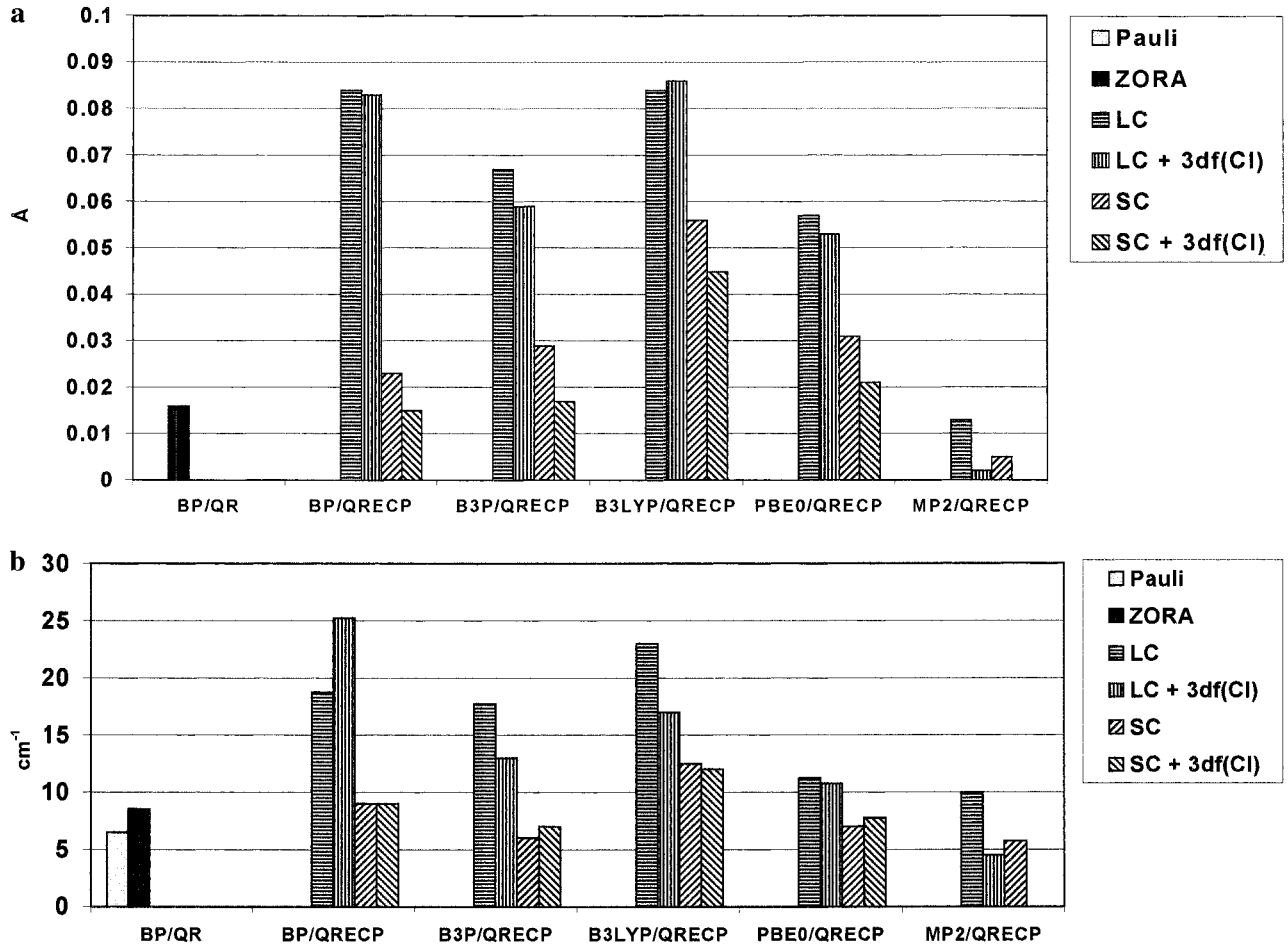

Figure 4. (a) Absolute mean deviations (in Å) of DFT and MP2 calculated bond lengths with respect to MP2/QRECP-SC+3df(Cl) computations. (b) Absolute mean deviations (in cm^{-1}) of DFT and MP2 calculated harmonic frequencies with respect to MP2/QRECP-SC+3df(Cl) computations.

emphasizing again the difficulty to compare thermal-averaged and equilibrium structures.

The effect of the inclusion or not of additional polarization functions (3df) on chlorine atoms among LC-QRECP calcula-

tions is weak on both structural and vibrational parameters. Except for B3LYP results, a small shortening of the bond lengths is observed, varying between 0.001 Å (BP) and 0.011 Å (MP2). Irregular changes in the bonding angles can be noted as well. These variations are usually less than 1°, with the exceptions of the B3P and B3LYP angles that exhibit stronger and decreasing deviations of 4.6° and 3.4°, respectively. Not surprisingly, the vibrational analysis is strongly correlated to these structural changes. We calculated a wavenumber absolute mean deviation that varies between 1 cm^{-1} (BP and PBE0) and 5 cm^{-1} (MP2). Higher but still small variations are observed for B3P and B3LYP calculations, i.e., 11 and 9 cm^{-1}, respectively. This can be easily explained by the influence of the bonding angle decrease on the out-of-plane bending mode.

A similar comparison between SC-QRECP results—including or not additional polarization functions on chlorine atoms—emphasizes these trends. Small bond shortenings are systematically observed, varying between 0.005 Å (MP2) and 0.012 Å (B3P) while bond angles slightly decrease (less than 1°). Correspondingly, the wavenumber absolute mean deviations are very small, less than 3 and 6 cm^{-1} for DFT and MP2 results, respectively.

Finally, it should be mentioned that several attempts were made to perform CCSD or MP4(SDQ) calculations in order to assess the convergence of our reference MP2 results. But it must be stressed that these high-level open-shell calculations are extremely demanding in terms of computer resources, especially for memory and disk storage. For instance, 50 MP4 optimizations cycles on one Compaq EV67 processor (667 MHz) took 5 days of CPU time, with 17 Gb disk space. From a practical point of view, we were not able to obtain an optimized geometry from either MP4 or CCSD calculations, a problem that may be due to instability in the numerical gradient-driven procedure employed.

Uranium Trimethyl Molecules. In a second step, we decided to calculate the optimized molecular parameters for another model molecule, i.e., the UMe_3 species. Unfortunately, no estimated or experimental data are available in the literature for this gas-phase complex. However, previous complete active space (CAS-SCF) calculations were carried out for this molecule in a valence double-ζ basis set employing relativistic effective core potentials for the uranium atom.[57] The authors compared their calculated molecular parameters with the X-ray data of the large $U[CH(SiMe_3)_2]_3$ organoactinide compound.[68] In our study, DFT/QR, DFT/QRECP, and MP2/QRECP calculations have been carried out. Both U−C bond lengths and C−U−C bond angles (θ) have been optimized, keeping the methyl groups frozen in a regular tetrahedral arrangement with a global C_{3v} geometry. Among the different possible methyl conformations, the following structure was found to be the most stable.

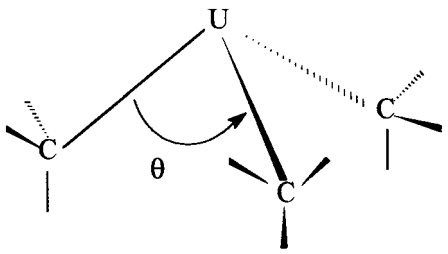

In Table 5, we compare our optimized geometries with the previous CAS-SCF calculations and the experimental solid-state structure of $U[CH(SiMe_3)_2]_3$. Although a systematic comparison between the $U(CH_3)_3$ and $U[CH(SiMe_3)_2]_3$ geometries is meaningless, a qualitative discussion is however possible. The DFT and MP2 calculated bond lengths are situated within a range of 2.35−2.47 Å. If we compare these results with the experimental U−C bond lengths of the $U[CH(SiMe_3)_2]_3$ complex, we notice that the calculated U−C distances of the uranium trimethyl molecule are shorter than the corresponding distances (2.48 Å) of this larger complex. Moreover, the $U(CH_3)_3$ molecule exhibits a more pronounced pyramidal structure, characterized by smaller θ bond angles (less than 100°). These bond lengths and angle variations are correlated to the size of the ligands. The bulky $CH(SiMe_3)_2$ groups induce strong steric interactions between them while weak repulsions characterize the methyl group interactions. Although a direct comparison between MP2/DFT and CAS-SCF calculations is not possible (different basis sets and pseudopotentials), it is however interesting to notice that the CAS-SCF calculations do not point this tendency out. Finally, a systematic comparison of the different DFT approaches used can be carried out. On the basis of the previous UX_3 results, we decided to choose the MP2 structure as a reference geometry and to compare the different calculated bond lengths. The best agreement is obtained with DFT/QR (ZORA) with a small deviation of 0.02 Å while the PBE0/QRECP and B3P/QRECP approaches present also a rather good agreement with bond length deviations of 0.03 and 0.04 Å, respectively. Higher deviations (>0.05 Å) are observed for other density functional calculations.

TABLE 5: Comparison between the Calculated Optimized Geometries of $U(CH_3)_3$ Molecules (U−C bond lengths in Å and C−U−C bond angles in degrees) and the Experimental Solid State Structure of $U[CH(SiMe_3)_2]_3$

molecule	method	*r*	θ
$U(CH_3)_3$	BP/QR/Pauli	2.352	97.5
	BP/QR/ZORA	2.382	97.6
	BP/QRECP	2.456	93.4
	B3P/QRECP	2.442	94.6
	B3LYP/QRECP	2.468	94.8
	PBE0/QRECP	2.440	94.8
	MP2/QRECP	2.406	91.5
	CAS-SCF[a]	2.543	105.6
$U[CH(SiMe_3)_2]_3$	exptl[b] (solid)	2.48	107.7

[a] Ref 57. [b] Ref 68.

Discussion. In this study, we have examined the influence of two essential components of heavy metal computations, i.e., the choice of the treatment of electron exchange and correlation and the treatment of relativistic effects by means of quasi-relativistic approximations. Clearly the use of a quasi-relativistic Hamiltonian, either in the Pauli or ZORA formalism, leads to the most satisfactory results, in the DFT framework. It should be noted that the ZORA approach gives a slightly better agreement than the Pauli formalism. Nevertheless, the difference is small between both approaches: this is most likely due to the fact that a frozen core has been used in both cases and that only valence electrons are involved, thus limiting the deficiency of the Pauli formalism to describe electrons close to the nucleus.

The LC-QRECP combined with DFT approaches give definitely a less interesting performance. For instance, the same gradient correction (BP) leads to a much better agreement with a Pauli or ZORA treatment than with the use of a LC-QRECP while the same number of valence electrons is treated. The use of hybrid functionals slightly improves the situation, as already observed by Hay and Martin[20] for similar but closed-shell systems. Nevertheless, the best performance with LC-QRECP is obtained in the post-HF MP2 methodology. This general result is at variance with the conclusions obtained by several studies on LnX_3 homologues, using a DFT formalism either with Dolg[19]

or Stevens et al.[17,18] LC-QRECP, compared with several other post-HF studies. It had been shown that the combination of QRECP with hybrid functionals was able to provide as good performance as post-HF methods such as MP2 or configuration interaction calculations. The less satisfying behavior of the DFT/LC-QRECP combination in the case of actinide-containing molecules compared with a MP2/LC-QRECP approach may possibly be related to the fact that the QRECP has been primarily derived from—and for—ab initio methods. The performance when used in the DFT formalism may still be satisfying with Ln compounds, but it deteriorates with heavier elements such as actinides.

In contrast, we have confirmed that a SC-QRECP scheme significantly decreases the deviations between DFT and MP2 calculations, this effect being more pronouced for a functional GGA. These results are in agreement with previous studies realized on U(VI) systems.[15,16,27] However, we would like to point out that the use of SC-QRECP is much more time-consuming for open-shell molecules and could be doubtfully adapted for larger practical systems. However, an interesting and promising alternative is the use of LC correlation-consistent basis sets, recently developed by Martin and Sundermann for other heavy elements (p-block).[69]

Among the DFT/LC-QRECP approaches, the various performances observed in that study follow the trends generally observed: the hybrid functionals give better agreement with experimental/estimated data than the simple gradient correction, and moreover, the PBE0 functional is the best among the SCH methods, whereas the worst is B3LYP. This deficiency may be related to the inadequacy of the LYP correlation functiona—as already mentioned above—to properly treat open-shell molecular systems (see refs 18, 23, and 52−54) while satisfactory results may be obtained for other heavy metal closed-shell systems.[16,19,20,27] Similar trends are observed as well with SC-QRECP.

4. Conclusion

In this paper, we have presented the first systematic structural and vibrational MP2/DFT study of UX_3 (X = F, Cl, Br, and I) and $U(CH_3)_3$ vapor molecules. On one hand, an ab initio MP2/LC-QRECP approach satisfactorily reproduces both estimated/experimental structures and spectroscopic data of these compounds. However, this approach demands a high computational effort. On the other hand, we have clearly shown that DFT/QR approaches are able to provide calculated molecular parameters very close from both MP2 (LC or SC) and DFT/SC-QRECP results but at a lower computational cost. Finally, the ZORA approach has been found to provide, as expected, a slightly better agreement with MP2/LC-QRECP or experimental/estimated data. The study of other actinide analogues or larger molecular systems is now under way, focusing on the description of lanthanide(III)/actinide(III)−ligand interactions.

Acknowledgment. It is a pleasure to thank Pr. Carlo Adamo (Ecole Nationale Supérieure de Chimie de Paris—France) for helpful discussions and providing PBE/PBE0 routines. We also thank the "Direction des Etudes Nucleaires", i.e., the Nuclear Studies Division of the Commissariat à l'Energie Atomique (France) for financial support.

References and Notes

(1) Cotton, S. *Lanthanides and Actinides*; MacMillan: London, 1991.
(2) *Handbook on the Physics and Chemistry of Rare Earths*; Gschneider, K. A., Jr., Eyring, L., Bernal Máquez, S., Eds.; Elsevier: Amsterdam, 1978−2000; Vol. 1−29.
(3) Kaltsoyannis, N.; Scott, P. *The f Elements*; Oxford University Press: Oxford, 1999.
(4) Durand, S.; Dognon, J.-P.; Guilbaud, P.; Rabbe, C.; Wipff, G. *J. Chem. Soc., Perkin Trans. 2* **2000**, 705.
(5) Baaden, M.; Wipff, G.; Yaftian, M. R.; Burgard, M.; Matt, D. C.; Schurhammer, R.; Matt, D. *J. Chem. Soc., Perkin Trans. 2* **2000**, 1315.
(6) Baaden, M.; Berny, F.; Madic, C.; Wipff, G. *J. Phys. Chem. A* **2000**, *104*, 7659.
(7) Baaden, M.; Berny, F.; Boehme, C.; Schurhammer, R.; Wipff, G. *J. Alloys Compd.* **2000**, *303−304*, 104.
(8) Dolg, M.; Stoll, H. *Handbook on the Physics and Chemistry of Rare Earths*; Gschneider, K. A., Jr., Eyring, L., Eds.; Elsevier: Amsterdam, 1996; Vol. 22, Chapter 152.
(9) Lanza, G.; Fragalà, I. L. *Chem. Phys. Lett.* **1996**, *255*, 341.
(10) Lanza, G.; Fragalà, I. L. *J. Phys. Chem. A* **1998**, *102*, 7990.
(11) Kovacs, A.; Konings, R. J. M.; Booij, A. S. *Chem. Phys. Lett.* **1997**, *268*, 207.
(12) Joubert, L.; Picard, G.; Legendre, J. *J. Inorg. Chem.* **1998**, *37*, 1984.
(13) Tsuchiya, T.; Taketsugu, H.; Nakano, K.; Hirao, J. *J. Mol. Struct. (THEOCHEM)* **1999**, *461−462*, 203.
(14) Dognon, J.-P.; Durand, S.; Granucci, G.; Levy, B.; Millie, P.; Rabbe, C. *J. Mol. Struct. (THEOCHEM)* **2000**, *507*, 17.
(15) Vallet, V.; Schimmelpfennig, B.; Maron, L.; Teichteil, C.; Leininger, T.; Gropen, O.; Grenthe, I.; Wahlgren, U. *Chem. Phys*. **1999**, *244*, 185.
(16) Ismail, N.; Heully, J.-L.; Saue, T.; Daudey, J.-P.; Marsden, C. J. *Chem. Phys. Lett*.
(17) Adamo, C.; Maldivi, P. *Chem. Phys. Lett.* **1997**, *268*, 61.
(18) Adamo, C.; Maldivi, P. *J. Phys. Chem. A* **1998**, *102*, 6812.
(19) Joubert L.; Picard G.; Legendre J.-J. *J. Alloys Compd*. **1998**, *275−277*, 934.
(20) Hay, P. J.; Martin, R. L. *J. Chem. Phys.* **1998**, *109*, 3875.
(21) Zhou, M.; Andrews, L.; Ismail, N.; Marsden, C. *J. Phys. Chem. A* **1998**, *104*, 5495.
(22) Schreckenbach, G.; Hay, P. J.; Martin, R. L. *J. Comput. Chem.* **1999**, *20*, 70.
(23) Vetere, V.; Adamo, C.; Maldivi, M. *Chem. Phys. Lett.* **2000**, *325*, 99.
(24) Maron, L.; Eisenstein, O. J. *Phys. Chem. A* **2000**, *104*, 7140.
(25) Cosentino, U.; Villa, A.; Pitea, D.; Moro, G.; Barone, V. *J. Phys. Chem A* **2000**, *104*, 8001.
(26) Tsushima, S.; Suzuki, A. *J. Mol. Struct. (THEOCHEM)* **2000**, *529*, 21.
(27) Han, Y.-K.; Hirao, K. *J. Chem. Phys.* **2000**, *113*, 7345.
(28) For a recent review on this subject, see, for example: Niu, S.; Hall, M. B. *Chem. Rev.* **2000**, *100*, 353.
(29) Snijders, J. G.; Baerends, E. J.; Ros, P. *Mol. Phys.* **1979**, *38*, 1919.
(30) Ziegler, T.; Tschinke, V.; Snijders, J. G.; Ravenek, W. J. *Phys. Chem.* **1989**, *93*, 3050.
(31) van Lenthe, E.; Baerends, E. J.; Snijders, J. G. *J. Chem. Phys.* **1993**, *99*, 4597.
(32) Baerends, E. J.; Ellis, D. E.; Ros, P. *Chem. Phys.* **1973**, *2*, 41.
(33) Versluis, L.; Ziegler, T. *J. Chem. Phys.* **1988**, *88*, 322.
(34) te Velde, G.; Baerends, E. J. *J. Comput. Phys.* **1992**, *99*, 84.
(35) Fonseca Guerra, C.; Snijders, J. G.; te Velde, G.; Baerends, E. J. *Theor. Chem. Acc.* **1998**, *99*, 391.
(36) Snijders, J. G.; Vernooijs, O.; Baerends, E. J. *At. Data Nucl. Data Tables* **1982**, *26*, 483.
(37) Krijn, J.; Baerends, E. J. *Internal Report, V. U.*, Amsterdam, 1984.
(38) Frisch, M. J.; Trucks, G. W.; Schlegel, H. B.; Scuseria, G. E.; Robb, M. A.; Cheesman, J. R.; Zakrzewski, V. G.; Montgomery, J. A.; Stratmann, R. E.; Burant, J. C.; Daprich, S.; Millam, J. M.; Daniels, A. D.; Kudin, K. N.; Strain, M. C.; Farkas, O.; Tomasi, J.; Barone, V.; Cossi, M.; Cammi, R.; Mennucci, B.; Pomelli, C.; Adamo, C.; Clifford, S.; Ochterski, J.; Petersson, G. A.; Ayala, P. Y.; Cui, Q.; Morokuma, K.; Malick, D. K.; Rabuck, A. D.; Raghavachari, K.; Foresman, J. B.; Cioslowski, J.; Ortiz, J. V.; Stefanov, B. B.; Liu, G.; Liashenko, A.; Piskorz, P.; Komaromi, I.; Gomperts, R.; Martin, R. L.; Fox, D. J.; Keith, T.; Al-Lahan, M. A.; Peng, C. Y.; Nanayakkora, A.; Gonzalez, C.; Challacombe, M.; Gill, P. M. W.; Johnson, B. G.; Chen, W.; Wong, M. W.; Andres, J. L.; Head-Gordon, M.; Replogle, E. S.; Pople, J. A. *Gaussian 98 (Revision A7)*; Gaussian Inc.: Pittsburgh, PA, 1998.
(39) Kuechle, W. To be published.
(40) Bergner, A.; Dolg, M.; Stoll, H.; Preuss, H. *Mol. Phys.* **1993**, *80*, 1431.
(41) Wood, J. H.; Boring, A. M. *Phys. Rev. B* **1978**, *18*, 2701.
(42) Møller, P.; Plesset, M. S. *Phys. Rev.* **1934**, *46*, 618.
(43) Frisch, M. J.; Pople, J. A.; Binkley, J. S. *J. Chem. Phys.* **1984**, *80*, 3265.
(44) Hariharan, P. C.; Pople, J. A. *Theor. Chim. Acta* **1973**, *28*, 213.
(45) Becke, A. D. *Phys. Rev. A* **1988**, *38*, 3098.
(46) Perdew, J. P. *Phys. Rev. B* **1986**, *33*, 8822.
(47) Becke, A. D. *J. Chem. Phys.* **1993**, *98*, 5648.
(48) Adamo, C.; Barone, V. *J. Chem. Phys.* **1999**, *110*, 6158.

(49) Lee, C.; Yang, W.; Parr, R. G. *Phys. Rev. B* **1988**, *37*, 785.
(50) Perdew, J. P.; Burke, K.; Ernzerhof, M. *Phys. Rev. Lett.* **1996**, *77*, 3865.
(51) Perdew, J. P.; Burke, K.; Ernzerhof, M. *Phys. Rev. Lett.* **1997**, *78*, 1396.
(52) McCullough, E. A., Jr.; Aprà, E.; Nichols, J. *J. Phys. Chem. A* **1997**, *101*, 2502.
(53) Redfern, P. C.; Blaudeau, J.-P.; Curtiss, L. A. *J. Phys. Chem. A* **1997**, *101*, 8701.
(54) Groen, C. P; Oskam, A. *Inorg. Chem.* **2000**, *39*, 6001.
(55) Crosswhite, H. M.; Crosswhite, H.; Carnal, W. T.; Pasze, A. P. *J. Chem. Phys.* **1980**, *72*, 5103.
(56) (a) Jones, E. R., Jr; Hendricks, M. E.; Stone, J. A.; Karraker, D. G. *J. Chem. Phys.* **1974**, *60*, 2088. (b) Berger, M.; Sienko, M. J. *Inorg. Chem.* **1967**, *6*, 324.
(57) Ortiz, J. V.; Hay, P. J.; Martin, R. L. *J. Am. Chem. Soc.* **1992**, *114*, 2736.
(58) Bazhanov, V. I.; Ezhov, Yu. S.; Komarov, S. A. *Zh. Strukt. Khim.* **1990**, *31*, 152.
(59) Bazhanov, V. I.; Ezhov, Yu. S.; Komarov, S. A. *Mol. Strukt.* **1990**, 109.
(60) Bazhanov, V. I.; Komarov, S. A.; Sevast'yanov, V. G.; Popik, M. V.; Kuznetsov, N. T.; Ezhov, Yu. S. *Vysokochist. Veshchestva* **1990**, *1*, 109.
(61) Kovács, A.; Booij, A. S.; Cordfunke, E. H. P.; Kok-Scheele, A.; Konings, R. J. M. J. Alloys Compd. **1996**, *241*, 95.
(62) Fuger, J.; Parker, V. B.; Hubbard, W. N.; Oetting, F. L. *The Chemical Thermodynamics of Actinide Elements and Compounds*, *Part 8*, *The Actinide Halides*; International Atomic Energy Agency: Vienna, 1983.
(63) Hildenbrand, D. L.; Gurvich, L. V.; Yungman, V. S. *The Chemical Thermodynamics of* Actinide Elements and Compounds, Part 13, The Gaseous Actinide Ions; International Atomic Energy Agency: Vienna, 1985.
(64) Hargittai, M. *Chem. Rev.* **2000**, *100*, 2233.
(65) *Handbook of Chemistry and Physics*; Weast, R. C., Ed.; CRC Press: Boca Raton, FL, 1985.
(66) Hauge, R. H.; Hastie, J. W.; Margrave, J. L. *J. Less-Common Met.* **1971**, *23*, 359.
(67) Hastie, J. W.; Hauge, R. H.; Margrave, J. L. *J. Less-Common Met.* **1975**, *39*, 309.
(68) Van Der Sluys, W. G.; Burns, C. J.; Sattelberg, A. P. *Organometallics* **1989**, *8*, 855.
(69) Martin, J. M. L.; Sundermann, A. *J. Chem. Phys.* **2001**, *114*, 3408.